

# Enhanced performance of VO<sub>x</sub>-based bolometer using patterned gold black absorber

Evan M. Smith,<sup>a,b,\*</sup> Deep Panjwani,<sup>a</sup> James Ginn,<sup>b</sup> Andrew Warren,<sup>b</sup> Christopher Long,<sup>b</sup> Pedro Figuiereido,<sup>a,b</sup> Christian Smith,<sup>a</sup> Joshua Perlstein,<sup>b</sup> Nick Walter,<sup>c</sup> Carol Hirschmugl,<sup>c</sup> Robert E. Peale,<sup>a</sup> David Shelton<sup>b</sup>

<sup>a</sup>Department of Physics, University of Central Florida, Orlando FL 32816

<sup>b</sup>Plasmonics, Inc., 12605 Challenge Pkwy STE 150, Orlando FL 32826

<sup>c</sup>Department of Physics, University of Wisconsin-Milwaukee, Milwaukee, WI 53211

## ABSTRACT

Patterned highly absorbing gold black film has been selectively deposited on the active surfaces of a vanadium-oxide-based infrared bolometer array. Patterning by metal lift-off relies on protection of the fragile gold black with an evaporated oxide, which preserves gold black's near unity absorption. This patterned gold black also survives the dry-etch removal of the sacrificial polyimide used to fabricate the air-bridge bolometers. Infrared responsivity is substantially improved by the gold black coating without significantly increasing noise. The increase in the time constant caused by the additional mass of gold black is a modest 14%.

**Keywords:** VO<sub>x</sub> bolometer, gold black, absorber, MEMS

## 1. INTRODUCTION

Infrared bolometers function by converting IR incident power into heat, which causes a measureable change in resistance. Devices are typically optimized for mid-wave IR (MWIR, 3-5 μm wavelength) or long-wave IR (LWIR, 8-12 μm wavelength) by Fabry-Perot<sup>1,2</sup> and other resonant structures,<sup>3-5</sup> whose peak absorbance and bandwidth depend on resonator Q and hence on fabrication tolerances. In contrast, gold black is a well-known absorber with very high absorption over a broad spectral range,<sup>6</sup> and which is easily deposited using an ordinary thermal evaporator. Thus, a multiband sensor can be fabricated using a single material with minimal fabrication tolerances. On the other hand, gold black is an extremely fragile material that until recently could not be effectively patterned for use on large-scale detector arrays.

Gold black is a porous, nano-crystalline structured gold film, achieved by depositing gold in ~1 Torr of an inert gas. The low mean free path inside the vacuum chamber causes gold atoms to collide and bind with each other prior to being deposited on the substrate.<sup>7</sup> This very low density material is extremely fragile, which makes it difficult to integrate into a micro-bolometer array, since usual fabrication processes destroy the film.

Some of us recently succeeded in patterning gold black using evaporated SiO<sub>2</sub> as a protection layer.<sup>8,9</sup> Meanwhile, Plasmonics, Inc. has developed high-performance room-temperature air-bridge bolometers based on VO<sub>x</sub>-Au thin films.<sup>10</sup> In this paper, we report successful integration of patterned gold black onto such a bolometer array, which resulted in a substantial improvement in detector performance.

## 2. THEORY

Voltage responsivity  $R_v$  is the change in measured voltage with incident power, given by<sup>10</sup>

$$R_v = \frac{V_B \alpha \eta}{4G_{eff}} \frac{1}{\sqrt{1 + \omega^2 \tau^2}}, \quad (1)$$

---

\* Corresponding author, email: [evansmith@knights.ucf.edu](mailto:evansmith@knights.ucf.edu)

where  $V_B$  is the applied bias voltage,  $\eta$  the absorptivity,  $G_{eff}$  the effective thermal conductance,  $\omega$  the modulation frequency,  $\tau$  the thermal time constant, and  $\alpha$  the Temperature Coefficient of Resistivity (TCR), defined as

$$TCR \equiv \alpha = \frac{1}{R} \frac{dR}{dT} . \quad (2)$$

Responsivity, therefore, can be increased in only a few ways. An increase of bias voltage will also cause an undesired increase in Johnson noise. Much work has been done already to increase the TCR of  $VO_x$ , which has reached a level of  $\sim 2\text{-}3\%$ .<sup>2</sup> Thermal conductance in air-bridge bolometers can be decreased at the expense of thermal time constant and mechanical stability. Increasing absorptivity based on various optical or plasmonic resonances can increase responsivity without increasing noise or thermal time constant, in principle. We previously reported a  $VO_x$  air-bridge bolometer with Fabry-Perot resonance absorption at LWIR wavelengths of 64%,<sup>10</sup> as determined by numerical calculation. The opportunity investigated in this paper is that a gold black coating can increase the absorptivity to 90%, giving a 40% increase in responsivity.

### 3. EXPERIMENTAL DETAILS

For characterization of absorptance, protected gold black films were fabricated on gold-coated silicon substrates following procedures described in Ref. [8]. Specular and diffuse reflectance spectra were measured in a Hemispherical Directional Reflectance Spectrometer (HDR) with unpolarized light at incidence angles of 7°, 15°, 30°, 45° and 60°. Measured transmission was confirmed to be zero due to the gold film on the silicon substrate.

Bolometer design and fabrication is described in Ref. [10]. Some changes to feature size and material thickness were made to enhance performance, increase structural stability, and improve the production yield. A 2.5  $\mu\text{m}$  resonant cavity enhances LWIR absorption, whose value was estimated by numerical electrodynamic calculation to be  $\sim 64\%$ . The vanadium oxide ( $VO_x$ ) active element was co-sputtered with gold to improve the TCR and encapsulated in  $SiO_2$  to protect it during etching. The structure is built upon a sacrificial polyimide pillar. Structural legs and electrical connection for the air bridges are Nichrome (80/20).

Gold black is deposited and patterned by standard lift-off technique according to Refs. [8,9]. Gold source material is thermally evaporated in a  $\sim 1$  Torr  $N_2$  ambient. The substrate with photolithographic resist pattern aligned to the bolometer array is thermoelectrically cooled. Then, 250 nm of  $SiO_2$  is deposited by electron beam evaporation. Lift-off of the films is done by submerging the sample in acetone for 10 minutes without any agitation. Then the sacrificial polyimide is removed in a Branson P3000 barrel asher using an isotropic oxygen plasma, during which temperatures exceed 80°C. The  $SiO_2$  layer successfully protects the gold black during this process. For testing purposes, one wafer containing hundreds of detectors was fabricated. A quarter of these were processed without the gold black coating as the baseline for comparison. Samples with and without gold black have very similar resistances and nearly identical  $VO_x$ -Au films. The detectors studied with and without gold black had resistance deviations less than 1%. Witness samples indicate a TCR variation less than 5%.

To test the absorption of individual fabricated pixels, we used the imaging spectrometer at the University of Wisconsin Milwaukee.<sup>11</sup> A Bruker Vertex FT-IR spectrometer with Hyperion 3000IR microscope was used to image the sample with a standard global source. A Focal Plane Array (FPA) detector allowed for spectral imaging with better than 1  $\mu\text{m}$  spatial sampling. The spectral resolution was 4  $\text{cm}^{-1}$  and the spectral range was 900-3700  $\text{cm}^{-1}$  (2.7-11.1  $\mu\text{m}$ ).

Free-standing bolometers are wire bonded to standard chip carriers using gold wire onto the gold bond pads on the wafer. These chip carriers are then placed in a vacuum box with wired feedthroughs, which allows for individual pixels to be measured externally while the box is evacuated. This box is pumped down to below 20 mTorr to limit thermal conduction via air molecules and placed a distance  $r$  away from a blackbody source (IR-301 Infrared Systems Development Corporation). An optical chopper located close to the blackbody modulates the signal. The detector is DC biased from a low-noise power source. An impedance-matched resistor is placed in series with the detector, and the detector is referenced with a lock-in amplifier and a spectrum analyzer. The signal on the detector is given by<sup>12</sup>

$$P_i(T) = \Delta L(T) \frac{A_{BB} A_d}{r^2} F_f \tau, \quad (3)$$

where  $A_{BB}$  is the area of the blackbody (26.4 cm<sup>2</sup>),  $A_d$  is the area of the detector,  $r$  is 18cm,  $\tau$  is the transmission of the window of the detector housing, and  $F_f$  is the form factor to convert a peak-to-peak signal to RMS values ( $\frac{\sqrt{2}}{\pi}$ ). The window is a Thallium Bromo-Iodide window, which has a transmission of ~70% from 0.6-40  $\mu\text{m}$ . The radiance term  $\Delta L$  is determined by evaluating Planck's Law in the wavelength range of the window,

$$L = + \frac{2k^4 T^4}{h^3 c^2} \int_{x_2}^{x_1} \frac{x^3}{e^x - 1} dx, \quad x = \frac{hc}{\lambda kT}. \quad (4)$$

Samples were tested at blackbody temperatures of 300°C, which correspond to incident powers of 44.43 nW in the 0.6-40  $\mu\text{m}$  window, or 9.89 nW in the 8-12  $\mu\text{m}$  bandwidth, according to Eqs. 3 and 4. Tests were run for ten samples without the gold black coating first to establish a baseline. Eight devices with the gold black coating were tested for comparison.

Bolometer signal was measured as a function of detector resistance with the chopping frequency at 80 Hz. The applied bias was 1 V. The signal was measured on a spectrum analyzer and confirmed with a lock-in amplifier using an integration time of 30 ms.

The detector noise was measured in a manner described in the ASTM standard for NETD measurements.<sup>13</sup> The incident power from the blackbody source is blocked by a shield. This shield is highly reflecting on the side facing the blackbody so as to not absorb heat, and it is highly emissive on the side facing the detector. The signal voltage is measured across the detector using the lock-in amplifier with an integration time constant of 10 s, 1 s, 30 ms and 1 ms. The signal voltage with the blackbody blocked is the noise.

To test for the effects of gold black on the thermal time constant of the detector, the signal is measured as a function of chopping frequency  $f$ . According to Eq. 1, the responsivity of the device is functionally dependent upon the modulation frequency of the incident power. In the derivations above, it was assumed that the chopping frequency is much slower than the inverse of the thermal time constant, therefore it may be ignored. However, at high chopping frequency the signal will fall off according to

$$S \propto \frac{1}{\sqrt{1+(2\pi f)^2 \tau^2}}. \quad (5)$$

#### 4. RESULTS

Protected gold black has high absorption in the mid-wave IR and long-wave IR.<sup>8</sup> Figure 1 presents new the reflectance spectra  $R$  for a gold black layer with 250 nm SiO<sub>2</sub> protection measured at a 7° angle of incidence. A minimum reflectance of just under 7% occurs at 9.4  $\mu\text{m}$  wavelength. The diffuse reflectance is < 1 % in the LWIR and only ~ 1% at MWIR wavelengths. Thus, the absorptance 1- $R$  of the gold black film is 70% in the long-wave IR with a peak of 93% at 9.4  $\mu\text{m}$ , and it is 84% in the mid-wave IR with a peak of 94% at 3  $\mu\text{m}$ .

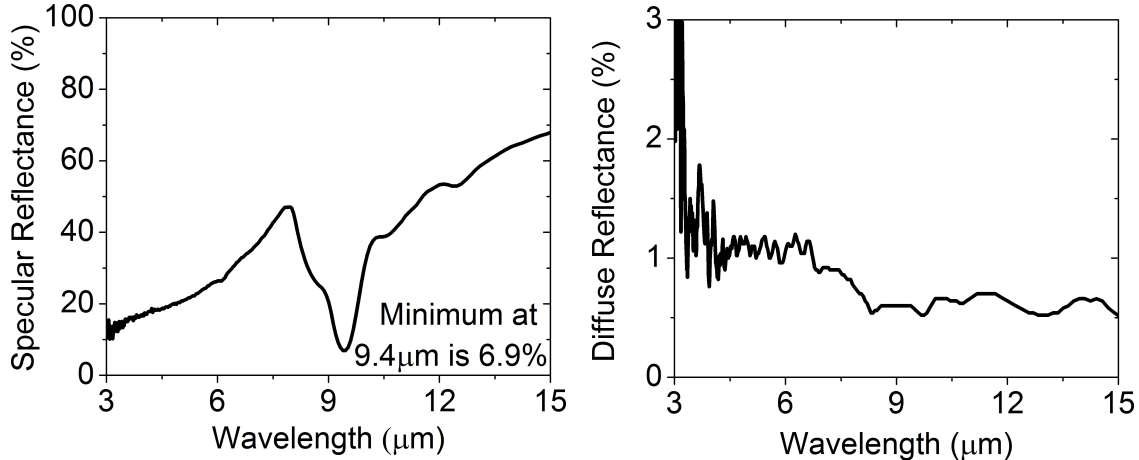


Figure 1. (left) HDR specular reflectance spectrum for gold black with 250 nm SiO<sub>2</sub> protection layer at 7° incident angle. (right) Diffuse reflectance of gold black film shows very little scattering in the 8-12 μm region.

Figure 2 presents scanning electron microscope images (SEM) of the air-bridge bolometers with and without gold black. The 35 μm x 35 μm square pixel elements appear rectangular because of the oblique view. The gold black appears as a thick furry carpet, but because its density is only ~8% that of bulk gold, it adds little to the heat capacity of each element.

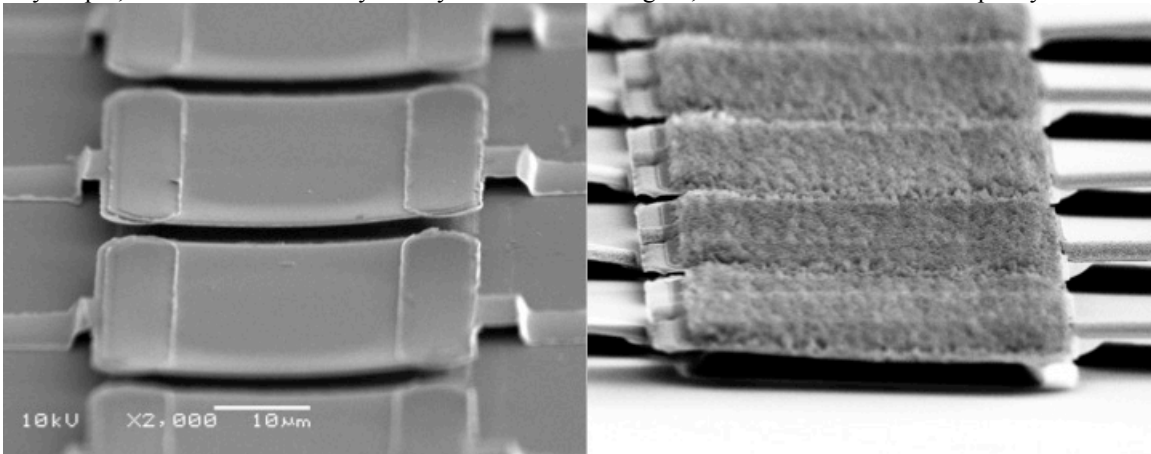


Figure 2. Bolometer pixels fabricated without (left) and with (right) gold black coating for comparison.

Fig. 3 presents a top-down SEM image of a linear bolometer array. There is slight misalignment of the gold black on the square resistor elements, but not enough to cause thermal or electrical cross talk between pixels or short to the substrate.

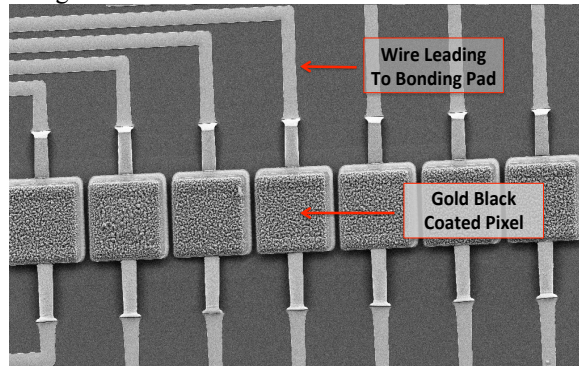


Figure 3. Array of free-standing air bridge bolometers patterned with gold black.

Absorbance spectral imaging on individual pixels is presented in Figure 4 (left). Reflectance spectra extracted from the central region in the spectral images of the bolometer are presented in Fig. 4 (right). The Fabry-Perot resonance is apparent between 8 and 10  $\mu\text{m}$  wavelengths, where the maximum absorbance without gold black is only 64%, in very good agreement with the numerical calculations. For pixels with gold black, the absorbance is  $\sim 90\%$  across the spectrum.

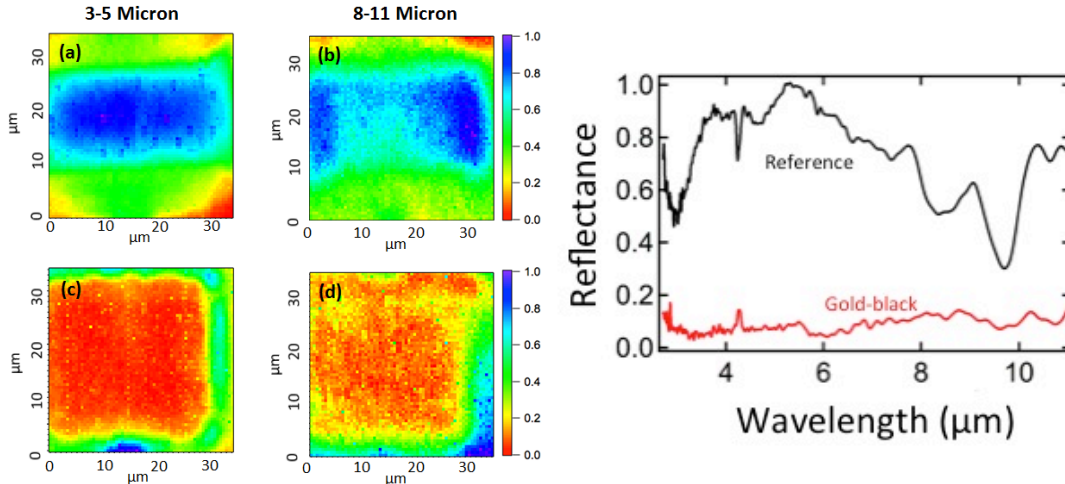


Figure 4. (left) IR reflectance spectral image of reference (a,b) and gold black coated (c,d) pixels. Spectral integrations are over MWIR (a,c) and LWIR (b,d) bands. Blue indicates the highest reflectance and red the lowest. (right) Infrared reflectance spectra R extracted from a portion of the spectral image near the center of the bolometer element with and without gold black.

Measured signal as a function of detector resistance is presented in Figure 5 (left). The average signal voltage for the reference samples is 40.6  $\mu\text{V}$ , while the average signal voltage of the gold black samples is 58.1  $\mu\text{V}$ , which represents an increase of 43% from the reference samples. There is some variance in the signal from pixel to pixel, as well as an inherent uncertainty in the measurement value of  $\pm 2 \mu\text{V}$ , but the signal from gold black coated samples is clearly much higher than for samples without gold black.

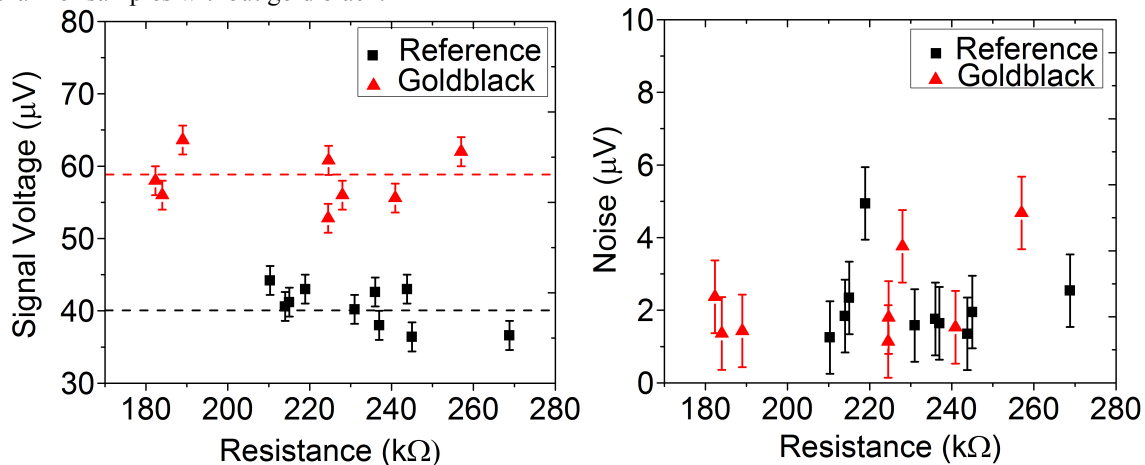


Figure 5. (left) Signal and (right) noise with and without gold black.

Noise data presented in Figure 5 (left) show no statistically significant difference for bolometers with and without gold black. The average noise for the reference samples is 2.12  $\mu\text{V}$ , while the gold black samples have an average noise of 2.26  $\mu\text{V}$ , a 7% difference, which is much less than the 40% uncertainty. A small increase in photon noise might be expected due to larger absorption bandwidth for gold black samples,<sup>14</sup> but these bolometers are not photon noise limited. From Figs. 5, we find that gold black provides a 43% increase in the signal to noise ratio (SNR), and a corresponding improvement in  $D^*$ .

Figure 6 (left) presents signal voltage versus chopping frequency. At each frequency, the gold black sample has approximately 40% more signal than the reference sample, as was seen in Fig. 5. A similar drop in signal with chopping frequency is observed with and without gold black, indicating little effect of gold black on the thermal time constant. The bolometers with and without gold black tested here had a resistances 242 and 240 k $\Omega$ , respectively.

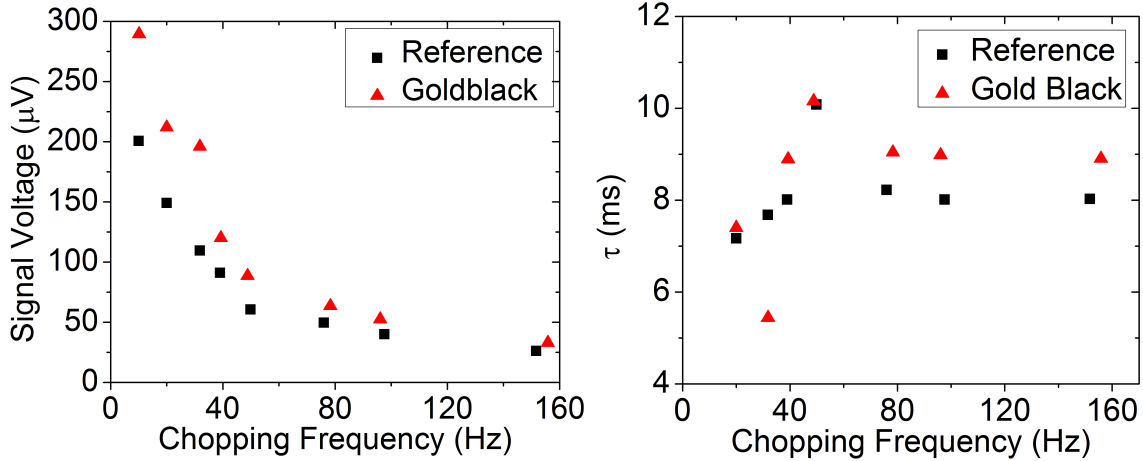


Figure 6. (left) Signal voltage and (right) thermal time constant as a function of chopping frequency for bolometers with and without gold black.

Calculated heat capacity of devices studied was  $1.28 \times 10^{-9} \text{ J K}^{-1}$  and thermal conductivity was  $5.83 \times 10^{-7} \text{ W m}^{-1} \text{ K}^{-1}$ . The density of the protected gold black after lift-off was estimated to be 8% of bulk gold, so 2  $\mu\text{m}$  thick gold black with 250 nm of  $\text{SiO}_2$  should add  $0.866 \times 10^{-9} \text{ J K}^{-1}$  to the heat capacity, giving a 68% increase. The thermal time constant is the ratio of the heat capacity to the thermal conductivity, so that we predict  $\tau = 2.17$  and 3.69 ms for bolometers without and with for the gold black. The relationship between signal and time constant Eq. 5 can be normalized as

$$S_{norm} = \frac{1}{\sqrt{1+(2\pi f\tau)^2}}, \quad (6)$$

where  $S_{norm} = 1$  represents the maximum signal when  $f\tau \ll 1$ . This condition holds at 10 Hz. Solving Eq. 6 for the time constant gives

$$\tau = \frac{1}{2\pi f \sqrt{S_{norm}^2 - 1}}. \quad (7)$$

A plot of  $\tau$  as a function of chopping frequency is presented in Fig. 6 (right). The  $\tau$  values should be functions of materials and geometry, independent of chopping frequency, but we observe some variation and the indication of a peak at 50 Hz. Averaging over all frequencies gives a thermal time constant without gold black of 8.29 ms and with gold black a value of 9.43 ms. The value without gold black is  $\sim 4$ x larger than the theoretical estimate, which may be explained by a thinner than expected metallization at the elbow joints of the bridge arms. With the measured thermal time constant of 8.29 ms and a heat capacity of  $1.28 \times 10^{-9} \text{ J K}^{-1}$ , we find a thermal conductance of  $1.54 \times 10^{-7} \text{ W m}^{-1} \text{ K}^{-1}$  for the reference sample. This thermal conductance should be the same for the gold black sample, except that the increase in  $\tau$  with gold black is much smaller than expected. These questions are still to be investigated.

Using measured time constants and the smaller thermal conductance just estimated, the signal voltage is calculated for both the reference films and the gold black film. As the primary absorption band is between 8-12  $\mu\text{m}$ , incident power only within this bandwidth is considered, which amounts to 9.89 nW. For the reference films, the absorption is taken to be 44% (as measured above), and with gold black it is 86%. The vanadium oxide film produced for these detectors has a TCR of  $-2.3\%/^\circ\text{C}$ . A 1V bias is also considered. The signal voltage for the reference detector is calculated to be 36.5  $\mu\text{V}$ , compared to the measured average of 40.6  $\mu\text{V}$ . The gold black sample has a calculated signal voltage of 63.1  $\mu\text{V}$ , compared to the measured average of 58.1  $\mu\text{V}$ . These values give voltage responsivities of 4.11 and 5.87  $\text{kV/W}$ , respectively.

## 5. SUMMARY

We have successfully patterned oxide-hardened gold black on a vanadium oxide bolometer using standard lift-off techniques. Measurements of these detectors show that the detector responsivity increases by 43% due to the increased absorption. Noise is unchanged. The time constant increases by 14%. In addition to increased signal and detectivity over a specific bandwidth, the addition of gold black absorbers negates the need for specific cavity spacing and increases the detector bandwidth, allowing for both mid-wave IR and long-wave IR capabilities.

## ACKNOWLEDGMENTS

This research was supported by a grant from the US Army Research Labs (ARL) SBIR program. We would also like to acknowledge the support and assistance from Mr. Guy Zummo, Mr. Ed Dein and Prof. Kevin Coffey.

## REFERENCES

- [1] Hunter, S.R., Amantea, R.A., Goodman, L.A., Kharas, D.B., Gershtein, S., Matey, J.R., Perna, S.N., Yu, Y., Maley, N., and White, L.K. "High Sensitivity Uncooled Microcantilever Infrared Imaging Arrays," Proc. SPIE 5074, 469-480 (2003).
- [2] Niklaus, F., Vieider, C., and Jakobsen, H., "MEMS-Based Uncooled Infrared Bolometer Arrays-A Review," Proc. SPIE 6836, 68360D (2007).
- [3] Liu, N., Mesch, M., Weiss, T., Hentschel, M., and Giessen, H. "Infrared Perfect Absorber and Its Application As Plasmonic Sensor," Nano Lett. 10(7), 2342-2348 (2010).
- [4] Watts, C.M., Liu, X., and Padilla, W. J. "Metamaterial Electromagnetic Wave Absorbers," Adv. Mater. 24(23), 98-120 (2012).
- [5] Ogawa, S., Komoda, J., Masuda, K., and Kimata, M. "Wavelength Selective Wideband Uncooled Infrared Sensor Using a Two-dimensional Plasmonic Absorber," Proc. SPIE 8704, 8704181-8704186 (2013).
- [6] Becker, W., Fettig, W.R., Gaymann, A., and Ruppel, W. "Black Gold Deposits as Absorbers for Far Infrared Radiation," Phys. Stat. Sol. (B) 194, 241-255 (1996).
- [7] Panjwani, D. [Metal Blacks as Scattering Centers to Increase Efficiency of Thin Film Solar Cells], Masters Thesis, UCF, Orlando (2011).
- [8] Panjwani, D., Yesiltas, M., Nath, J., Maukonen, D.E., Rezadad, I., Smith, E.M., Peale, R.E., Hirschmugl, C., Sedlmair, J., Wehlitz, R., Unger, M., and Boreman, G. "Patterning of Oxide-Hardened Gold Black by Photolithography and Metal Lift-off," Infrared Physics & Technology 62, 94-99 (2014).
- [9] Panjwani, D. "Infrared detector with metal-black coating having dielectric overlayer and related methods," U.S. Patent No. 20,140,374,597, 25 Dec. 2014.
- [10] Smith, E. M., Ginn, J.C., Warren, A.P., Long, C.J., Panjwani, D., Peale, R.E., Shelton, D.J. "Linear Bolometer array using a high TCR VO<sub>x</sub>-Au film," Proc. SPIE 9070, 90701Z (2014).
- [11] Nasse, M. J., Walsh, M.J., Mattson, E.C., Reininger, R., Kajdacsy-Balla, A., Macias, V., Bhargava, R., and Hirschmugl, C.J., "High Resolution Fourier-Transform Infrared Chemical Imaging with Multiple Synchrotron Beams," Nat. Methods 8, 413-416 (2011).
- [12] Dereniak, E. L. and Boreman, G. D., [Infrared Detectors and Systems], John Wiley and Sons, New York, (1996).
- [13] ASTM Standard E1543-00 (2012), "Standard Test Method for Noise Equivalent Temperature Difference of Thermal Imaging Systems," ASTM International, West Conshohocken, PA, 2012, DOI: 10.1520/E1543-00R11, [www.astm.org](http://www.astm.org)
- [14] Talghader, J. T., Gawarikar, A. S., Shea, R. P., "Spectral selectivity in infrared thermal detection," Light: Science and Applications 1(24), e24 (2012).